

# Double plasmonic nanodisks design for electromagnetically induced transparency and slow light

Gen Lai, Ruisheng Liang,\* Yujing Zhang, Zhenyu Bian, Lixuan Yi, Guangzhi Zhan, Ruitong Zhao

Guangdong Provincial Key Laboratory of Nanophotonic Functional Materials and Devices, School for Information and Optoelectronic Science and Engineering, South China Normal University, Guangzhou 510006, China

\*liangrs@scnu.edu.cn

**Abstract:** An analog of plasmonic system for electromagnetically induced transparency (EIT), in which a small nanodisk with a big side-coupled-nanodisk is directly coupled to the metal-insulator-metal (MIM) waveguide, has been proposed and investigated theoretically and numerically. When the resonant frequencies of the two nanodisks differ not too much, a powerful EIT-like effect can be obtained, and the transparency window can be easily tuned by adjusting the radii of the two nanodisks. The plasmonic device can be used as a high-performance EIT-like filter with transmission over 80% and full width at half-maximum (FWHM) less than 30nm, besides, the novel structure shows a high group index over 355. The system paves a new way toward highly integrated optical circuits and networks, especially for wavelength-selective, ultrafast switching, light storage and nonlinear devices.

©2015 Optical Society of America

**OCIS codes:** (240.6680) Surface plasmons; (260.2110) Electromagnetic optics; (130.3120) Integrated optics devices.

---

## References and links

1. W. L. Barnes, A. Dereux, and T. W. Ebbesen, "Surface plasmon subwavelength optics," *Nature* **424**(6950), 824–830 (2003).
2. J. Park, H. Kim, and B. Lee, "High order plasmonic Bragg reflection in the metal-insulator-metal waveguide Bragg grating," *Opt. Express* **16**(1), 413–425 (2008).
3. B. Wang and G. P. Wang, "Plasmon Bragg reflectors and nanocavities on flat metallic surfaces," *Appl. Phys. Lett.* **87**(1), 013107 (2005).
4. H. Lu, X. M. Liu, D. Mao, and G. X. Wang, "Plasmonic nanosensor based on Fano resonance in waveguide-coupled resonators," *Opt. Lett.* **37**(18), 3780–3782 (2012).
5. T. S. Wu, Y. M. Liu, Z. Y. Yu, Y. W. Peng, C. G. Shu, and H. Ye, "The sensing characteristics of plasmonic waveguide with a ring resonator," *Opt. Express* **22**(7), 7669–7677 (2014).
6. H. Lu, X. M. Liu, L. Wang, Y. Gong, and D. Mao, "Ultrafast all-optical switching in nanoplasmonic waveguide with Kerr nonlinear resonator," *Opt. Express* **19**(4), 2910–2915 (2011).
7. G. Z. Zhan, R. S. Liang, H. T. Liang, J. Luo, and R. Zhao, "Asymmetric band-pass plasmonic nanodisk filter with mode inhibition and spectrally splitting capabilities," *Opt. Express* **22**(8), 9912–9919 (2014).
8. Y. Gong, X. Liu, and L. Wang, "High-channel-count plasmonic filter with the metal-insulator-metal Fibonacci-sequence gratings," *Opt. Lett.* **35**(3), 285–287 (2010).
9. K. J. Boller, A. Imamolu, and S. E. Harris, "Observation of electromagnetically induced transparency," *Phys. Rev. Lett.* **66**(20), 2593–2596 (1991).
10. S. E. Harris, J. E. Field, and A. Imamoglu, "Nonlinear optical processes using electromagnetically induced transparency," *Phys. Rev. Lett.* **64**(10), 1107–1110 (1990).
11. K. Totsuka, N. Kobayashi, and M. Tomita, "Slow light in coupled-resonator-induced transparency," *Phys. Rev. Lett.* **98**(21), 213904 (2007).
12. T. Baba, "Slow light in photonic crystals," *Nat. Photonics* **2**(8), 465–473 (2008).
13. Y. Huang, C. Min, and G. Veronis, "Subwavelength slow-light waveguides based on a plasmonic analogue of electromagnetically induced transparency," *Appl. Phys. Lett.* **99**(14), 143117 (2011).
14. L. Zhu, F. Y. Meng, J. H. Fu, Q. Wu, and J. Hua, "Multi-band slow light metamaterial," *Opt. Express* **20**(4), 4494–4502 (2012).

15. L. Dai, Y. Liu, and C. Jiang, "Plasmonic-dielectric compound grating with high group-index and transmission," *Opt. Express* **19**(2), 1461–1469 (2011).
16. H. Lu, X. M. Liu, and D. Mao, "Plasmonic analog of electromagnetically induced transparency in multi-nanoresonator-coupled waveguide system," *Phys. Rev. A* **85**(5), 053803 (2012).
17. Q. Xu, S. Sandhu, M. L. Povinelli, J. Shakya, S. Fan, and M. Lipson, "Experimental realization of an on-chip all-optical analogue to electromagnetically induced transparency," *Phys. Rev. Lett.* **96**(12), 123901 (2006).
18. J. J. Chen, C. Wang, R. Zhang, and J. Xiao, "Multiple plasmon-induced transparencies in coupled-resonator systems," *Opt. Lett.* **37**(24), 5133–5135 (2012).
19. V. Kravtsov, J. M. Atkin, and M. B. Raschke, "Group delay and dispersion in adiabatic plasmonic nanofocusing," *Opt. Lett.* **38**(8), 1322–1324 (2013).
20. G. Wang, "Slow light engineering in periodic-stub-assisted plasmonic waveguide," *Appl. Opt.* **52**(9), 1799–1804 (2013).
21. Z. Chen, W. H. Wang, L. N. Cui, L. Yu, G. Y. Duan, Y. F. Zhao, and J. H. Xiao, "Spectral Splitting Based on Electromagnetically Induced Transparency in Plasmonic Waveguide Resonator System," *Plasmonics* 1–7 (2014).
22. G. T. Cao, H. J. Li, S. P. Zhan, H. Xu, Z. Liu, Z. He, and Y. Wang, "Formation and evolution mechanisms of plasmon-induced transparency in MDM waveguide with two stub resonators," *Opt. Express* **21**(8), 9198–9205 (2013).
23. T. Wang, Y. S. Zhang, Z. Hong, and Z. H. Han, "Analogue of electromagnetically induced transparency in integrated plasmonics with radiative and subradiant resonators," *Opt. Express* **22**(18), 21529–21534 (2014).
24. G. T. Cao, H. J. Li, S. P. Zhan, Z. H. He, Z. B. Guo, X. K. Xu, and H. Yang, "Uniform theoretical description of plasmon-induced transparency in plasmonic stub waveguide," *Opt. Lett.* **39**(2), 216–219 (2014).
25. H. A. Haus and W. P. Huang, "Coupled-mode theory," *Proc. IEEE* **79**(10), 1505–1518 (1991).
26. Z. Han and S. I. Bozhevolnyi, "Plasmon-induced transparency with detuned ultracompact Fabry-Perot resonators in integrated plasmonic devices," *Opt. Express* **19**(4), 3251–3257 (2011).
27. X. S. Lin and X. G. Huang, "Tooth-shaped plasmonic waveguide filters with nanometric sizes," *Opt. Lett.* **33**(23), 2874–2876 (2008).
28. H. A. Haus, *Waves and fields in optoelectronics* (Prentice-Hall, New Jersey, 1984).
29. H. Lu, X. M. Liu, G. X. Wang, and D. Mao, "Tunable high-channel-count bandpass plasmonic filters based on an analogue of electro-magnetically induced transparency," *Nanotech.* **23**(44), 444003 (2012).
30. B. Tang, L. Dai, and C. Jiang, "Electromagnetic response of a compound plasmonic-dielectric system with coupled-grating-induced transparency," *Phys. Lett. A* **376**(14), 1234–1238 (2012).
31. I. Chremmos, "Magnetic field integral equation analysis of interaction between a surface plasmon polariton and a circular dielectric cavity embedded in the metal," *J. Opt. Soc. Am. A* **26**(12), 2623–2633 (2009).
32. C. Zeng, J. Guo, and X. M. Liu, "High-contrast electro-optic modulation of spatial light induced by graphene-integrated Fabry-Pérot microcavity," *Appl. Phys. Lett.* **105**(12), 121103 (2014).

## 1. Introduction

Surface plasmon polaritons (SPPs) are considered to have dramatically potential application in the realization of highly integrated optical circuits due to their capability to overcome the diffraction limit of light [1]. A large number of devices based on SPPs, such as Bragg reflectors [2,3], sensors [4,5], optical switching [6], filters [7,8] and so on, have been proposed and investigated experimentally or theoretically. Over these years, a novel phenomenon analogous to EIT found in dielectric photonic resonator systems has triggered another round of research in this field. EIT is a quantum interference phenomenon between the different excitation pathways to atomic levels which can be observed in atomic systems [9], and it has potential applications in the areas of nonlinearities [10], modulations and slowing light propagation [11,12]. However, The demanding experimental conditions required to observe the EIT effect are so difficult to serve that hinder its practical application. But the EIT-like optical responses obtained in classical plasmonic resonator systems are easily realized and integrated into the chips.

There are two ways for the generation of EIT-like effects: **the near-field coupling between modes of resonator directly coupled to waveguide and resonator not coupled to waveguide** [21,23]; **and the phase coupling between detuned resonators coupled to bus waveguide** [16,18,20,22,24]. We could find that there are lots of research about the EIT-like phenomenon both in theoretical prediction and experimental demonstration [13–23]. For example, Huang and associates used the transmission line theory and scattering matrix theory to introduce the subwavelength slow-light mode in periodic-stub-assisted plasmonic waveguides [13] and Cao et al. studied uniform theoretical description of plasmon-induced transparency in plasmonic stub waveguide [24]. Recently, Wang et al. demonstrated an analog of EIT in integrated

plasmonics with radiative and subradiant resonators [23]. However, most of the previous works were concentrated on plasmonic resonator systems with stub or/and FP waveguide. **There were very few or even no studies about analog of EIT in disk-resonator directly coupled to the bus waveguide with no stub. In addition, the preceding designs' transmission properties were not very well.**

In this paper, we propose a novel compact plasmonic waveguide system consisting of two different nanodisks, one of the nanodisk directly coupled to the MIM waveguide, and the other, big one, coupled to the small one with a gap. Comparing with most of the previous resonator systems with stub or/and FP waveguide, for example Ref [23], the circular resonators have high coupling coefficient and quality factor which is better for slowing light, besides, circular resonators is easy to be fabricated. The transmission properties of the system are simulated by finite-difference time-domain (FDTD) method with grid size  $5 \times 5$  nm. A coupled mode theory (CMT) [25,30] based on transmission line theory has been introduced to interpret this phenomenon and we found that this device shows a powerful EIT-like effect. The transparency window can be tuned by changing the geometrical parameters of the structure. And the physical mechanism is analyzed in detail. The proposed compact plasmonic structure may pave a new way for the high-performance EIT-like devices.

## 2. Theoretical analysis and discussion of MIM waveguide with one nanodisk resonator

Figure 1(a) shows the nanoscale plasmonic resonator system with one nanodisk directly coupled to a bus waveguide. This system is a two-dimensional model. The medium of the waveguide and nanodisk is assumed to be air ( $n = 1$ ) and the background material in blue is silver. The permittivity of silver is characterized by Drude model  $\epsilon(\omega) = \epsilon_\infty - \omega_p^2 / (\omega^2 + i\omega\gamma)$ , where  $\epsilon_\infty$  presents the permittivity at infinite angular frequency and is chosen as 3.7,  $\omega_p$  is the bulk plasma frequency with the value of 9.1eV and  $\gamma$  is the oscillation damping of electrons and the value is 0.018eV [26]. The width of the MIM waveguide and the radius of the disk are denoted by  $w$  and  $r$ , respectively.

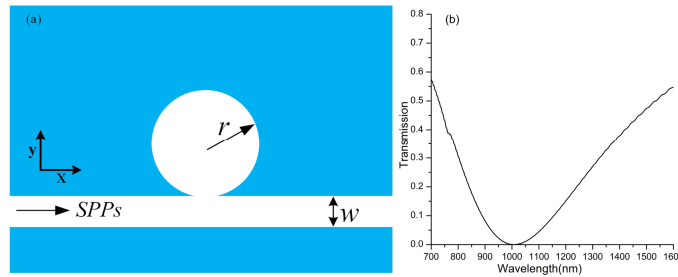


Fig. 1. (a) Schematic of MIM waveguide directly coupled to a nanodisk resonator with gap = 0. (b) Transmission spectra for MIM waveguide directly coupled to nanodisk, with  $w=50\text{nm}$  and  $r=70\text{nm}$ .

Figure 1(b) shows the transmission spectra for the MIM waveguide directly with one nanodisk resonator. We could find that it's a broadband stop filter and the transmission spectra line looks the same as a stub directly coupled to a MIM waveguide in [27]. The FDTD method with perfectly matched layer boundary conditions are used in the numerical experiment. By using the CMT [25,28], the transmission of the system supporting a resonant mode of frequency  $\omega_0$  can be expressed as

$$T = \frac{(\omega - \omega_0)^2 + \left(\frac{1}{\tau_0}\right)^2}{(\omega - \omega_0)^2 + \left(\frac{1}{\tau_0} + \frac{1}{\tau_e}\right)^2} \quad (1)$$

where  $\omega$  stands for the frequency of the incident light, and  $\omega_0$  is the resonance frequency of the nanodisk.  $1/\tau_0$  and  $1/\tau_e$  are the decay rate due to the intrinsic loss and the power escaping into the waveguide, respectively. It is obvious that the minimum transmission  $T_{\min}$ ,  $T_{\min} = (1/\tau_0)^2 / (1/\tau_0 + 1/\tau_e)^2$ , happens when  $\omega = \omega_0$ . As the size of the system is much small than the wavelength of the incident light, we neglected the intrinsic loss and got  $T_{\min} = 0$ , which does accord well with the CMT.

### 3. Electromagnetically-induced-transparency-like with two different nanodisks

The schematic illustration of the original plasmonic system we proposed is shown in Fig. 2(a). Figure 2(b) is the corresponding transmission spectra with  $w = 50\text{nm}$ ,  $g = 10\text{nm}$ ,  $r = 70\text{nm}$ , and  $R = 249\text{nm}$ . It can be clearly found that there is a typical and powerful EIT-like effect formed at  $1006\text{nm}$  which is also the resonator mode of the big nanodisk with  $R = 249\text{nm}$ . When

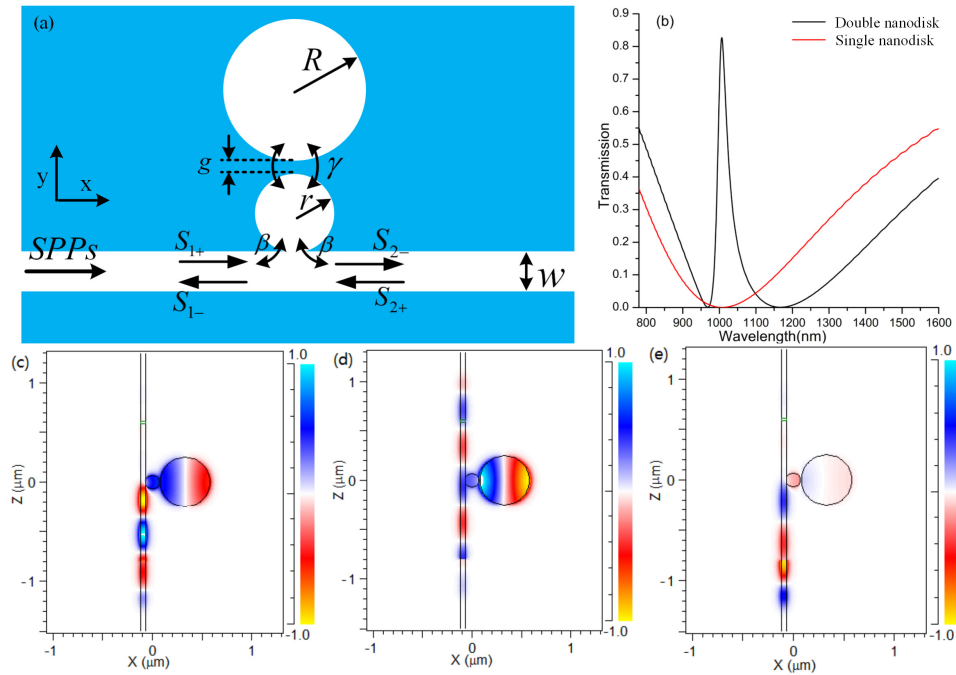


Fig. 2. (a) Schematic of MIM waveguide directly coupled to a small nanodisk and a big nanodisk couple to the small one with a gap. (b) Transmission spectra with single (red curve) and double (black curve) nanodisks. The parameters are set as  $w = 50\text{nm}$ ,  $g = 10\text{nm}$ ,  $r = 70\text{nm}$ ,  $R = 249\text{nm}$ . (c-e) Magnetic field distributions of the double nanodisks system at 968nm, 1006nm, 1168nm, respectively.

the small nanodisk resonator is coupled with the larger nanodisk resonator, a narrow transmission peak is formed in the broad stop-band of the single small resonator, and the transmission spectra at  $1006\text{nm}$  has increased from 0 to 82.7%. This is because the coherent

interference between the two optical pathways, namely, the direct excitation of resonant mode in the small disk by the incident wave and the excitation by coupling with larger nanodisk resonator [29]. In other words, the broad resonant mode of the small nanodisk is split into two resonant modes, one of them is blue shifted while the other is red shifted [21]. Figures 2(c)-2(e) show the magnetic field distributions of resonant modes at 968nm, 1006nm, 1168nm, respectively. We can see that the  $H_y$  fields in the directly coupled nanodisk is in-phase with the  $H_y$  fields in input MIM waveguides at 1006nm. It means that incident light and the light escaping into the bus waveguide from the nanodisk has a coherence enhancement. Nevertheless, the magnetic field distributions show that there is anti-phase between the small nanodisk and MIM waveguide at 968nm and 1168nm, namely, conditions of resonance destructive have been met then inhibit transmission of the waves. The magnetic intensity in the big nanodisk at 1168nm is so weak because the wave is far from the resonant mode.

In order to provide the detail theoretical analysis to illustrate the EIT-like phenomenon, we introduce a CMT-based transmission line theory [30]. As shown in Fig. 2(a), the coupling coefficient between the two nanodisk is denoted by  $\gamma$ . The small nanodisk directly coupled to a waveguide can be treated as an oscillator and the cavity mode decays equally into the propagating waveguide,  $\beta$  is the coupling coefficient between them. Here, we neglected the loss. The amplitude of the incoming and outgoing waves into the cavity denoted by  $S_{i+}$  and  $S_{i-}$  ( $i=1$  or  $i=2$ ), respectively and they are also normalized to the power carrier by the waveguide mode. When the electromagnetic wave at a frequency  $\omega$  is launched into the system from the input port of the bus waveguide, i.e.  $S_{2+}=0$ , the time evolution of the normalized amplitude  $a$  of small nanodisk and  $b$  of big nanodisk can be expressed as

$$\frac{da}{dt} = (j\omega_r - \beta - \gamma)a + j\sqrt{\beta}(S_{1+} + S_{2+}) + j\sqrt{\gamma}b \quad (2)$$

$$\frac{db}{dt} = j\omega_r b - \gamma b + j\sqrt{\gamma}a \quad (3)$$

Where  $\omega_r$ ,  $\omega_r$  is the resonant frequency of the small and big nanodisk, respectively.  $j = \sqrt{-1}$ . As the power conservation and the time reversal symmetry, the relationship between the amplitudes of the incoming and outgoing waves in the waveguides can be described as follows:

$$S_{2-} = S_{1+} + j\sqrt{\beta}a \quad (4)$$

$$S_{1-} = S_{2+} + j\sqrt{\beta}a \quad (5)$$

Using Eqs. (2)-(5), the transmission coefficient  $T$  into the output port at steady state can be determined as

$$T = \left| \frac{S_{2-}}{S_{1+}} \right|^2 = \left| \frac{j(\omega - \omega_r) + \gamma + \frac{\gamma}{[j(\omega - \omega_r) + \gamma]}}{[j(\omega - \omega_r) + (\beta + \gamma)] + \frac{\gamma}{[j(\omega - \omega_r) + \gamma]}} \right|^2 \quad (6)$$

From Eq. (6), we can quantitatively and clearly comprehend the forming of EIT-like phenomenon: as incident optical waves transmit into this system, wave with frequency of  $\omega_r$  will be suppressed and no transmission when there is only the small nanodisk. Adding the big

nanodisk with resonant frequency  $\omega_R = \omega_r$ , the transmission  $T$  is becoming  $\left| \frac{\gamma+1}{\beta+\gamma+1} \right|^2$ , which means a transparency window emerging. From Eq. (6), we can also find and explain that there would be EIT-like effect happened at frequency  $\omega = \omega_R$  as long as the  $\omega_r$  and  $\omega_R$  not differ each other too much, and the corresponding transmittance is  $\left| \frac{j(\omega_R - \omega_r) + \gamma + 1}{j(\omega_R - \omega_r) + \beta + \gamma + 1} \right|^2$ .

#### 4. Transmission properties of the proposed structure with different parameters

As we have theoretically presented that there are also EIT-like phenomenon appeared with changing  $\omega_R$  in a certain scope. In this part, we investigated the transmission properties with different  $R$  and  $g$ .

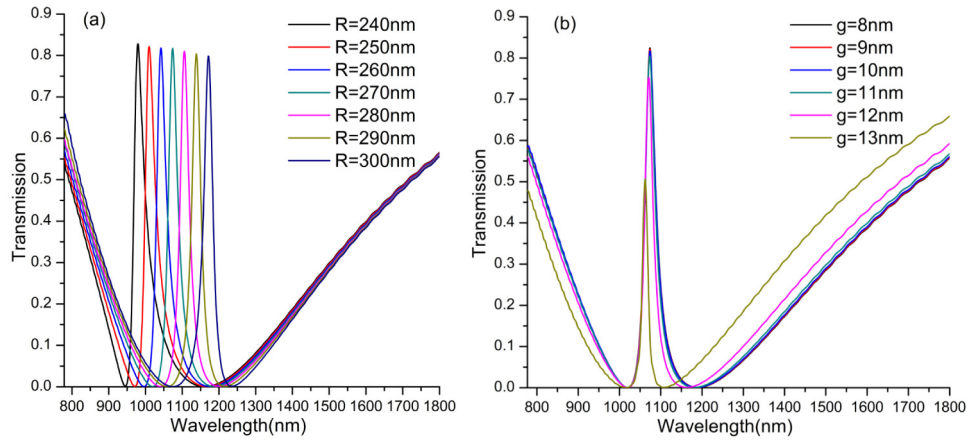


Fig. 3. (a) Transmission spectra for different radii of the larger nanodisk cavity with  $r = 70\text{nm}$ ,  $g = 10\text{nm}$ ,  $w = 50\text{nm}$ . (b) Transmission spectra for different gap between the two nanodisk with  $r = 70\text{nm}$ ,  $R = 270\text{nm}$ ,  $w = 50\text{nm}$ .

Figure 3(a) shows the transmission spectra with different radii of the larger nanodisk. Here we changed the resonant frequency of the big nanodisk through changing its radius, and there relationship can be obtain from [7,31]. It is obvious that the resonance peak wavelength has a red shift with the increasing of  $R$ , radius of the big nanodisk, and the corresponding transmission present a decline because of increasing loss. We can make the transparency widow happens at any wavelength. For example, we want it forming among 950nm to 1250nm, we just need to adjust parameter of  $R$ . If we want it happening out of this range, we should tune the radii both of the two nanodisk to make sure that  $\omega_r \approx \omega_R = \omega$ ,  $\omega$  denotes the wavelength you want.

We also found that this device could be used as a high-performance optical filter. The blue line of Fig. 4(d) shows the FWHM with different  $R$ . When  $r = 70\text{nm}$ ,  $R = 270\text{nm}$ ,  $g = 10\text{nm}$ , the corresponding maximum transmittance at 1074nm is 81.7% and its FWHM is 29.7nm. As two of the most important indexes of filter after making a trade-off they are better than most of previous optical filters. For example, though there is a EIT-like peak over 90% in [32], however, it shows much more broad FWHM than ours. Figure 3(b) shows transmission spectra and Fig. 4(e) presents FWHM for different gap between the two nanodisks with  $r = 70\text{nm}$ ,  $R = 270\text{nm}$ ,  $w = 50\text{nm}$ , respectively. We can clearly find that the maximum transmittance present a tendency of decline and have a ultra-narrow FWHM as the increase of  $g$ . There is a tradeoff when we construct this device. We can obtain filter at any wavelength through tuning parameters  $r$  and  $R$ .

## 5. Slow-light effect of this structure

It is well known that EIT-like phenomenon can support slow group velocities, and the slow-light effect can be described by the group index  $n_g$ , which is calculated from the dispersion of the phase as follows [16]:

$$n_g = \frac{c}{v_g} = \frac{c}{L} \tau_g = \frac{c}{L} \cdot \frac{d\psi(\omega)}{d\omega} \quad (7)$$

Where  $v_g$  is the group velocity in the plasmonic waveguide systems.  $\tau_g$  and  $\psi(\omega)$  are the optical delay time and transmission phase shift, respectively.  $L$  stands for the length of plasmonic system.

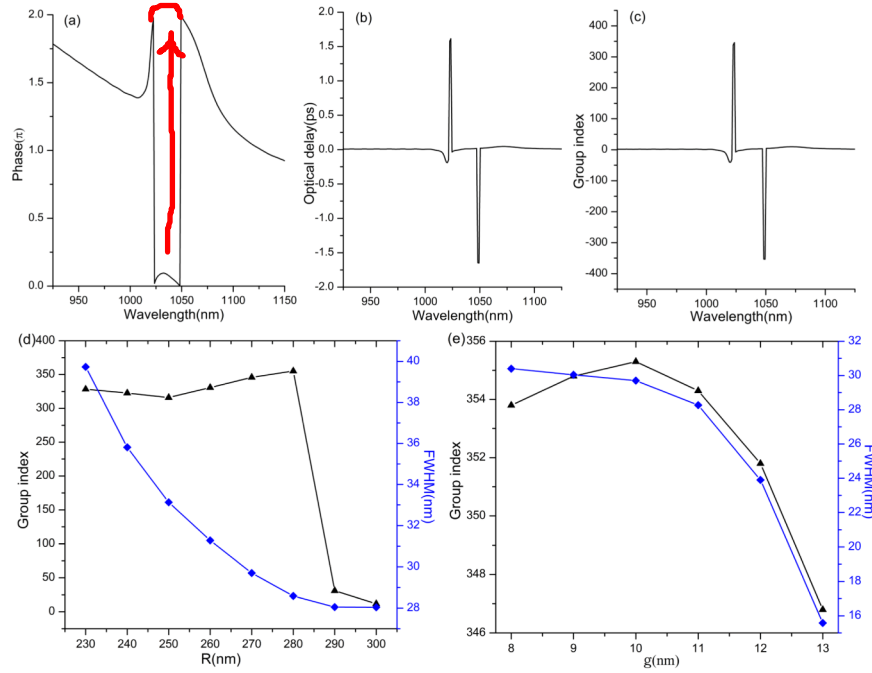


Fig. 4. (a) Transmission phase shift, (b) optical delay line, and (c) group indices in the plasmonic system with  $r = 70\text{nm}$ ,  $R = 270\text{nm}$ ,  $g = 10\text{nm}$ . (d) and (e) are the corresponding maximum group indices and FWHM with different  $R$  from 230nm-300nm under  $g = 10\text{nm}$  and with different  $g$  from 8nm-13nm at  $R = 280$ , respectively.

We numerically investigated the slow-light behavior in this structure with  $r = 70\text{nm}$ ,  $R = 270\text{nm}$ ,  $g = 10\text{nm}$ . Figure 4(a) shows the phase shift from the optical source to the detector and we can find that phase slope is steepest at the location of the EIT-like peak. It's different from the conventional dispersion curve because most of the previous works were focus on stub coupled to bus waveguide, however, nanodisk has different coupling coefficient and properties with the stub. This plasmonic system exhibits the large optical delay in the transparency window, with a maximum delay time of about 1.6ps at the corresponding transparency window as shown in Fig. 4(b). The group indices are depicted in Fig. 4(c). High group indices around the transparency peak result from the strong dispersion in the transparency window. The maximum group index is over 345 at the transparency-peak wavelength.

In order to get more insight about the slow-light effect in our system. We investigated the relationship between the group indices and  $R$ ,  $g$ , respectively. We could find that the group

index dramatically decline when  $R \geq 280\text{nm}$  result from  $\omega_l$  and  $\omega_r$  differ with each other too much and we could find that there happened the red shift mode around  $R = 290\text{nm}$  from Fig. 3(a) so the EIT-like effect is weak. We could also clearly see from Fig. 4(e) that  $g = 10\text{nm}$  is the best to slow light. The maximum group index is over 355 with a group velocity  $v_g \approx 0.0028c$  of achieved. which is promising for the development of ultra-compact slow light devices.

## 6. Conclusion

In summary, a novel plasmonic EIT-like system which consists of two nanodisks side-coupled to MIM bus waveguide has been proposed and investigated theoretically and numerically. We found that the EIT-like phenomenon can be achieved when the resonant frequencies of the small nanodisk and big nanodisk differ not too much. The desired transparency window can be tuned by adjusting the radii of the two nanodisks. The CMT-based transmission line theory is well coupled with the FDTD results. This plasmonic system can be used as a high-performance filter, besides, our ultracompact configurations can realize group indices over 355 as well as retain high peak transmission. This novel plasmonic system has important potential applications in highly integrated optical circuits and networks, especially for wavelength-selective, ultrafast switching, light storage and nonlinear devices.

## Acknowledgments

This work was supported by the National Natural Science Foundation of China Grants No.61275059 and No.61307062.